HHS Public Access

Author manuscript

Biochemistry. Author manuscript; available in PMC 2019 March 27.

Published in final edited form as:

Biochemistry. 2018 March 27; 57(12): 1833–1837. doi:10.1021/acs.biochem.8b00010.

Neutron Crystallography Detects Differences in Protein Dynamics: Structure of the PKG II Cyclic Nucleotide Binding Domain in Complex with an Activator

Oksana Gerlits[†], **James C. Campbell**[‡], **Matthew P. Blakeley**[§], **Choel Kim**[*,‡,‖], and **Andrey Kovalevsky**[⊥,*]

[†]Bredesen Center, University of Tennessee, Knoxville, Tennessee 37996, United States

[‡]Department of Pharmacology and Chemical Biology, Baylor College of Medicine, Houston, Texas 77030, United States

[§]Large-Scale Structures Group, Institut Laue Langevin, 38042 Grenoble Cedex 9, France

[‖]Verna and Marrs McLean Department of Biochemistry and Molecular Biology, Baylor College of Medicine, Houston, Texas 77030, United States

[⊥]Neutron Scattering Division, Neutron Sciences Directorate, Oak Ridge National Laboratory, Oak Ridge, Tennessee 37831, United States

Abstract

As one of the main receptors of a second messenger, cGMP, cGMP-dependent protein kinase (PKG) isoforms I and II regulate distinct physiological processes. The design of isoform-specific activators is thus of great biomedical importance and requires detailed structural information about PKG isoforms bound with activators, including accurate positions of hydrogen atoms and a description of the hydrogen bonding and water architecture. Here, we determined a 2.2 Å room-temperature joint X-ray/neutron (XN) structure of the human PKG II carboxyl cyclic nucleotide binding (CNB-B) domain bound with a potent PKG II activator, 8-pCPT-cGMP. The XN structure directly visualizes intermolecular interactions and reveals changes in hydrogen bonding patterns upon comparison to the X-ray structure determined at cryo-temperatures. Comparative analysis of the backbone hydrogen/deuterium exchange patterns in PKG II:8-pCPT-cGMP and previously reported PKG Iβ:cGMP XN structures suggests that the ability of these agonists to activate PKG is

[*]Corresponding Authors: kovalevskyay@ornl.gov. Phone: +1 505 310 4184. ckim@bcn.edu. Phone: +1 713 798 8411.

ORCID

Choel Kim: 0000-0002-3152-0020

Andrey Kovalevsky: 0000-0003-4459-9142

Notes

The authors declare no competing financial interest.

Author Contributions

J.C.C., C.K., and A.K. designed the research. O.G., J.C.C., and A.K. performed the research. A.K. and M.P.B. collected neutron diffraction data. O.G. and A.K. performed the structural analysis.

Supporting Information

The Supporting Information is available free of charge on the ACS Publications website at DOI: 10.1021/acs.biochem.8b00010. A detailed description of crystallization methods, X-ray and neutron data collection, joint X-ray/neutron refinement, Figure S1, and Table S1 containing crystallographic statistics (PDF)

related to how effectively they quench dynamics of the cyclic nucleotide binding pocket and the surrounding regions.

Cyclic GMP protein kinases (PKG) are crucial mediators of the nitric oxide-cGMP signaling pathway that regulates numerous physiological responses, including smooth muscle tone, nociception, memory formation, and bone growth.[1,2] Mammalian cells have two types of PKGs, isoforms I and II.[3,4] Each enzyme shows distinct subcellular localization, tissue expression, and substrates, suggesting their nonredundant cellular functions. PKG I and II isoforms contain tandem cyclic nucleotide binding domains (CNB-A and -B) that tightly regulate the kinase activity in cGMP-dependent manner.[5,6] Each CNB domain folds into an eight-stranded β barrel and has variable numbers of α helices.[7,8] The β barrel contains a highly conserved structural motif termed the phosphate binding cassette (PBC). Consisting of a short helix (P helix) and a loop, the PBC provides multiple contacts with the ribose cyclic phosphate of cGMP. PKG I and II show a large degree of sequence similarity (50% identical sequences) and comparable architecture for CNB domains.[9] The CNB domains demonstrate variable affinities and selectivities for cGMP. CNB-A domains of PKG I and II isoforms have little selectivity for cGMP over cAMP.[8,9] In contrast, the CNB-B domains are highly selective for cGMP and act as gatekeeper domains for the cGMP-dependent activation of each isoform.[9,10]

Recent crystal structures of PKG I CNB domains demonstrated that isoform-specific interactions observed between the CNB-B β5/αC helix and the guanine moiety of cGMP are responsible for their high cGMP selectivity.[8–11] In PKG Iβ, the guanine moiety interacts with Leu296 and Arg297 on the β5 strand through hydrogen bonds and forms π–π stacking interactions with Tyr351 of the αC helix. Unlike those of PKG I, isoform-specific interactions with the guanine are provided by Asp412 and Arg415 of the αC helix of the CNB-B domain in PKG II. Mutating these residues significantly reduces the level of cGMP binding and cGMP-dependent activation but has a negligible effect on the level of cAMP binding and cAMP-mediated activation. Nuclear magnetic resonance studies comparing different PKG Iβ CNB-B domain conformations in the apo, cAMP-bound, and cGMP-bound states demonstrated the significance of conformational dynamics.[12]

Several cGMP analogues are available for functional studies of PKG isoforms with different specificities.[13,14] For example, the analogue 8-(4-chlorophenylthio)guanosine 3′,5′-cyclic monophosphate [8-pCPT-cGMP (Scheme 1)] is the most potent activator for PKG II, while PKG I is more sensitive to β-phenyl-1,N^2-ethenoguanosine 3′,5′-monophosphate (PET-cGMP). However, these compounds are not specific: both can activate either isoform at low micromolar concentrations. Additionally, they can activate cAMP-dependent protein kinases (PKAs) and interact with cyclic nucleotide-gated channels and phosphodiesterases at high concentrations.

Despite the wide usage of the cGMP analogues in determining cellular functions of PKG isoforms, little is known about how these analogues interact with the different isoforms. Low-temperature (LT) X-ray crystallography is commonly used to study protein–ligand interactions at high resolution. However, room-temperature (RT) neutron structures suggest that some interactions inferred from LT X-ray structures as strong hydrogen (H) bonds are

weaker or missing in RT structures.[15,16] For example, our recent joint RT X-ray/ neutron (XN) structure of the PKG Iβ CNB-B domain bound to cGMP (PDB entry 4QXK) demonstrated that the key interactions of Arg297 with cGMP are more dynamic than what the LT X-ray structure suggested.[11] Here, to obtain direct information about hydrogen bonding interactions, we determined a RT XN structure of the human PKG II CNB-B domain bound with 8-pCPT-cGMP at 2.2 Å resolution [PDB entry 6BQ8 (Figure 1 and Table S1)]. This complex represents the first neutron structure of a CNB domain bound with a kinase activator. We compared the differences in binding of 8-pCPT-cGMP and cGMP to the PKG II CNB-B domain. We then analyzed the backbone hydrogen/deuterium (H/D) exchange patterns of the current PKG II structure and compared them with that in the previously determined PKG Iβ:cGMP neutron structure.[11] Our analysis suggests a correlation between the dynamics of the PBC and adjacent pockets and the activation potency of PKG agonists. We hypothesize that the activator's potency depends on its ability to efficiently decrease the overall dynamics of the binding pocket and may not be limited to its affinity for the site.

The bound 8-pCPT-cGMP is clearly visible in the neutron scattering length density map (Figure 1A) with its cGMP moiety captured between the P helix of the PBC and the β5 strand. The bulky chlorophenylthio (8-pCPT) moiety extends to the adjacent hydrophobic pocket lined by strand β4 and β5 and helix αC residues. Overall, the RT XN structure of the PKG II CNB-B:8-pCPT-cGMP complex agrees well with the previously published LT X-ray structures of the same domain bound with cGMP (PDB entry 5BV6)[9] and 8-pCPT-cGMP (PDB entry 5JIZ)[17] (root-mean-square deviation values of 0.54 and 0.57 Å, respectively, for the matching main chain atoms). The ribose phosphate of 8-pCPT-cGMP in the RT XN structure makes six direct hydrogen (H) bonds and one water-mediated interaction with the PBC at the cGMP binding pocket. The guanine moiety makes four direct H-bonds with Lys347, Ser367, and Asp412 and one water-mediated contact with Asp411. A major difference is that the H-bond formed by Lys347 is shorter in the RT XN structure than in the LT X-ray structure with cGMP (Figure 1A). The RT XN structure shows a distance of 2.8 Å between N_ζ of Lys347 and N7 of guanine compared to a distance of 3.2 Å in the PKG II CNB-B:cGMP complex, indicating stronger interaction with the analogue. This change is due to introduction of the 8-pCPT moiety at position C8 of guanine. The bulky 8-pCPT group pushes the side chain of Lys347 toward the guanine pocket and positions its ND_3^+ group closer to the N7 atom. The C_γ–C_δ–C_ε–N_ζ torsion angle changes from 162° to 78° upon 8-pCPT-cGMP binding (Figure 1A). In major contrast, the analogue-bound LT X-ray structure shows a C_γ–C_δ–C_ε–N_ζ torsion angle of −175° (Figure 1A), which indicates no interaction with guanine's N7 atom. This change in the LT structure is likely caused by cryocooling rather than 8-pCPT-cGMP binding. Thus, the relevance of side chain conformations found in LT structures to the protein function and ligand binding should be interpreted with care, as was discussed previously for HIV-1 protease[16] and human carbonic anhydrase.[18]

Our RT XN structure suggests that H bonds between Arg415 and the guanine C6 carbonyl group in 8-pCPT-cGMP are weaker than previously reported. Arg415 and Asp412 were recently identified as critical residues for achieving high cGMP selectivity by the CNB-B domain of the PKG II isoform. Mutating either of these residues increases its EC_{50} value for

cGMP.[9] In our RT XN structure, Asp412 forms two strong H-bonds with the amino group at C2 and N1 of guanine of 2.8 and 2.7 Å, respectively, accepting deuterium atoms from them. However, the guanidinium group of Arg415 is 3.3–3.4 Å from guanine's O6 atom. Arg415's D atoms are placed out of the plane containing nitrogen and oxygen atoms, indicating weak interactions between these groups. This might be a result of Arg415 providing unique crystal contacts (Figure 1B). The structure showed that Arg415 forms a salt bridge with Glu292 from the neighboring molecule in the crystal. The salt bridge, in turn, prevents Arg415 from forming strong hydrogen bonds with the guanine. Because mutating Arg415 indeed reduced its affinity for cGMP, this salt bridge is unlikely to exist in solution.

Binding of 8-pCPT-cGMP induces structural changes in the neighboring hydrophobic pocket. This pocket consists of residues from strands β5 and β6 (Lys347, Leu349, Tyr354, and Phe355), the PBC (Glu357), and helix αC (Tyr400, Tyr404, and Leu408). The most significant change is the repositioning of the Tyr404 side chain (Figure 2). The cGMP-bound structure showed an ordered water molecule trapped among Tyr355, Tyr404, and the OH group of the ribose. Both LT X-ray and RT XN structures of PKG II CNB-B:8-pCPT-cGMP showed that this water is missing and is displaced by the 8-pCPT moiety. Tyr404 moves away with its side chain rotating ~90° around the C_β–C_γ bond to avoid a steric clash with 8-pCPT. This places Tyr404 farther from Tyr354, creating a solvent-shielded cavity for the hydrophobic 8-pCPT group. Lastly, helix αC moves slightly away from the rest of the domain relative to its position in the PKG II CNB-B:cGMP complex to accommodate the 8-pCPT moiety.

Comparison of the RT XN structures of the current PKG II CNB-B:8-pCPT-cGMP and previous PKG I CNB-B:cGMP[11] complexes shows different H/D exchange patterns of the backbone amide hydrogens in the PBC. In particular, the PKG II:8-pCPT-cGMP complex shows that the amides of Glu357 and Lys358 at the P helix of the PBC are fully exchanged with deuterium, whereas no exchange was observed for the analogous residues, Glu307 and Lys308, in the PKG Iβ:cGMP complex (Figure 3). In the PKG II:8-pCPT-cGMP complex, the carboxylate group of Glu357 forms only one H-bond ($O_{\varepsilon 2}$ of Glu357 accepts a D atom from 2′-OH of ribose). The analogous residue in the PKG Iβ:cGMP complex, Glu307, forms four H-bonds. The ribose hydroxyl donates its deuterium to the O_ε1 atom of Glu307, while $O_{\varepsilon 2}$ makes hydrogen bonds with the side chain ND_3^+ of Lys308 and the hydroxyl of Tyr351. The $O_{\varepsilon 1}$ atom of Glu307 additionally interacts with its own main chain amide. These differences might explain the different extents of H/D exchange between the two complexes. While we expected similar H/D exchange patterns for the PBC in these two complexes due to their similar structures and exposure to solvent, the different H/D exchange patterns may reflect changes in the dynamics of the P helix in the nucleotide-bound state of the PKG I and II CNB-B domains. Our data suggest that, despite tighter binding of cGMP (EC_{50} values of cGMP are 31 nM for PKG II CNB-B and 215 nM for PKG I CNB-B)[9,10] or 8-pCPT-cGMP (260 nM for PKG II and 1.6 μM for PKG I) (Figure S1) to the PKG II CNB-B domain than to the PKG I domain, the P helix of PKG II is more dynamic than that of PKG I. Correct positioning and decreased dynamics of the PBC may be important for the activation of PKG isoforms. PBC positioning is controlled by interactions with the ribose cyclic phosphate, and disrupting these contacts prevents the conformational changes required for kinase activation as suggested in the inhibited state of PKG Iβ CNB-B

and PKA RIα.[19,20] It is less clear how dynamics influences the activation/inactivation events in the presence of activators and inhibitors. This is because, while enhanced PBC dynamics was detected for the CNB domains bound with partial agonists or antagonists of PKG and PKA with respect to the activator-bound state,[12,20] no data are available to evaluate the effect of different activators (cGMP, 8-pCPT-cGMP, PET-cGMP, etc.) on PBC dynamics. Additional areas with different H/D exchange patterns include β5 residues and residues lining the adjacent hydrophobic pocket (Figure 3 and Table S2). The PKG II:8-pCPT-cGMP complex shows less H/D exchange for these regions suggesting a reduced solvent accessibility and decreased dynamics. On the basis of these observations, we hypothesize that more efficient quenching of the binding pocket dynamics fine-tunes PKG II activation, which may explain the high activation potency of 8-pCPT-cGMP. The van der Waals contacts formed by the 8-pCPT group of the analogue further stabilize the activated conformation. The 8-pCPT moiety extends toward the αC helix and provides additional interactions between the αC helix and the rest of the CNB-B domain. These interactions may reduce the dynamics of the CNB-B domain compared to that of its cGMP-bound state (Figure 4). If this assumption is correct, the bulky substituent at position 8 is necessary for high-potency activation. Also, the addition of a hydrogen bond-accepting/ donating group to this position may increase the activator's specificity for PKG II, as opposed to its direct incorporation on the guanine moiety at position 8, as was previously suggested.[17] For 8-pCPT-cGMP, such a group can be placed at the ortho-to-chlorine position on the 8-pCPT moiety and could potentially interact with the side chain hydroxyl of a conserved Tyr404 located nearly at the αC helix.

To summarize, we have demonstrated the ability of neutron crystallography to critically assess H-bonding interactions, their geometry, and their relative strength compared to conventional cryo-crystallography. Comparison of H/D exchange patterns in PKG II:8-pCPT-cGMP and PKG Iβ:cGMP neutron structures allowed us to propose that the activation potency of different agonists might be related to their ability to effectively quench dynamics of the P helix or neighboring regions. Further studies are necessary to confirm or refute this hypothesis. Design of isoform-specific PKG activators is an important biomedical problem, which contrasts classical drug design, because potent activators may not necessarily have to bind the strongest. Protein dynamics may become a crucial piece of the puzzle in the design of potent activators, rather than inhibitors, as is the case for high-affinity drugs.

Supplementary Material

Refer to Web version on PubMed Central for supplementary material.

Acknowledgments

Funding

O.G. and A.K. were supported by the U.S. Department of Energy's (DOE) Office of Basic Energy Sciences. J.C.C. and C.K. were funded by National Institutes of Health Grant R01 GM090161. This work has been authored by UT-Battelle LLC under DOE Contract DE-AC05-00OR22725.

The authors thank Liying Qin and Shelton Boyd for critical reading of the manuscript. The research at Oak Ridge National Laboratory's High Flux Isotope Reactor (IMAGINE beamline) was sponsored by the Scientific User

Facilities Division, Office of Basic Energy Sciences, U.S. Department of Energy. The authors thank Institut Laue Langevin (beamline LADI-III) for awarded neutron beam time.

ABBREVIATIONS

PKG	cGMP-dependent protein kinase
PKA	cAMP-dependent protein kinase
CNB	cyclic nucleotide binding domain
PBC	phosphate binding cassette
PDB	Protein Data Bank

References

1. Francis SH, Busch JL, Corbin JD, Sibley D. cGMP-dependent protein kinases and cGMP phosphodiesterases in nitric oxide and cGMP action. Pharmacol Rev. 2010; 62:525–563. [PubMed: 20716671]
2. Feil R, Lohmann SM, de Jonge H, Walter U, Hofmann F. Cyclic GMP-Dependent Protein Kinase and the Cardiovascular System. Insights from Genetically Modified Mice. Circ Res. 2003; 93:907–916. [PubMed: 14615494]
3. Butt E, Geiger J, Jarchau T, Lohmann SM, Walter U. The cGMP-dependent protein kinase: gene, protein, and function. Neurochem Res. 1993; 18:27–42. [PubMed: 8385276]
4. Hofmann F, Bernhard D, Lukowski R, Weinmeister P. cGMP-regulated protein kinases (cGK). Handb Exp Pharmacol. 2009; 191:137–162.
5. Reed RB, Sandberg M, Jahnsen T, Lohmann SM, Francis SH, Corbin JD. Fast and Slow Cyclic Nucleotide-dissociation Sites in cAMP-dependent Protein Kinase Are Transposed in Type 1β cGMP-dependent Protein kinase. J Biol Chem. 1996; 271:17570–17575. [PubMed: 8663415]
6. Taylor MK, Uhler MD. The Amino-terminal Cyclic Nucleotide Binding Site of the Type II cGMP-dependent Protein Kinase Is Essential for Full Cyclic Nucleotide-dependent Activation. J Biol Chem. 2000; 275:28053–28062. [PubMed: 10864932]
7. Osborne BW, Wu J, McFarland CJ, Nickl CK, Sankaran B, Casteel DE, Woods VL Jr, Kornev AP, Taylor SS, Dostmann WR. Crystal structure of cGMP-dependent protein kinase reveals novel site of interchain communication. Structure. 2011; 19:1317–1327. [PubMed: 21893290]
8. Kim JJ, Casteel DE, Huang G, Kwon TH, Ren RK, Zwart P, Headd JJ, Brown NG, Chow DC, Palzkill T, Kim C. Co-crystal structures of PKG Iβ (92–227) with cGMP and cAMP reveal the molecular details of cyclic-nucleotide binding. PLoS One. 2011; 6:e18413. [PubMed: 21526164]
9. Campbell JC, Kim JJ, Li KY, Huang GY, Reger AS, Matsuda S, Sankaran B, Link TM, Yuasa K, Ladbury JE, Casteel DE, Kim C. Structural basis of cyclic nucleotide selectivity in cGMP-dependent protein kinase II. J Biol Chem. 2016; 291:5623–5633. [PubMed: 26769964]
10. Huang GY, Kim JJ, Reger AS, Lorenz R, Moon EW, Zhao C, Casteel DE, Bertinetti D, VanSchouwen B, Selvaratnam R, Pflugrath JW, Sankaran B, Melacini G, Herberg FW, Kim C. Structural basis for cyclic-nucleotide selectivity and cGMP-selective activation of PKG I. Structure. 2014; 22:116–124. [PubMed: 24239458]
11. Huang GY, Gerlits OO, Blakeley MP, Sankaran B, Kovalevsky AY, Kim C. Neutron diffraction reveals hydrogen bonds critical for cGMP-selective activation: insights for cGMP dependent protein kinase agonist design. Biochemistry. 2014; 53:6725–6727. [PubMed: 25271401]
12. VanSchouwen B, Selvaratnam R, Giri R, Lorenz R, Herberg FW, Kim C, Melacini G. Mechanism of cAMP partial agonism in protein kinase G (PKG). J Biol Chem. 2015; 290:28631–28641. [PubMed: 26370085]
13. Schwede F, Maronde E, Genieser HG, Jastorff B. Cyclic nucleotide analogs as biochemical tools and prospective drugs. Pharmacol Ther. 2000; 87:199–226. [PubMed: 11008001]

14. Schlossmann J, Hofmann F. cGMP-dependent protein kinases in drug discovery. Drug Discovery Today. 2005; 10:627–634. [PubMed: 15894227]

15. Weber IT, Waltman MJ, Mustyakimov M, Blakeley MP, Keen DA, Ghosh AK, Langan P, Kovalevsky AY. Joint X-ray/neutron crystallographic study of HIV-1 protease with clinical inhibitor amprenavir – insights for drug design. J Med Chem. 2013; 56:5631–5635. [PubMed: 23772563]

16. Gerlits O, Keen DA, Blakeley MP, Louis JM, Weber IT, Kovalevsky A. Room temperature neutron crystallography of drug resistant HIV-1 protease uncovers limitations of X-ray structural analysis at 100K. J Med Chem. 2017; 60:2018–2025. [PubMed: 28195728]

17. Campbell JC, Henning P, Franz E, Sankaran B, Herberg FW, Kim C. Structural basis of analog specificity in PKG I and II. ACS Chem Biol. 2017; 12:2388–2398. [PubMed: 28793191]

18. Kovalevsky A, Aggarwal M, Velazquez H, Cuneo MJ, Blakeley MP, Weiss KL, Smith JC, Fisher SZ, McKenna R. To be or not to be" protonated: atomic details of human carbonic anhydrase-clinical drug complexes by neutron crystallography and simulation. Structure. 2018; 26:383. [PubMed: 29429876]

19. Campbell JC, VanSchouwen B, Lorenz R, Sankaran B, Herberg FW, Melacini G, Kim C. Crystal structure of cGMP-dependent protein kinase Ib cyclic nucleotide-binding-B domain: R_P-cGMPS complex reveals an apo-like, inactive conformation. FEBS Lett. 2017; 591:221–230. [PubMed: 27914169]

20. Badireddy S, Yunfeng G, Ritchie M, Akamine P, Wu J, Kim CW, Taylor SS, Qingsong L, Swaminathan K, Anand GS. Cyclic AMP analog blocks kinase activation by stabilizing inactive conformation: conformational selection highlights a new concept in allosteric inhibitor design. Mol Cell Proteomics. 2011; 10:M110. 004390.

21. Ho BK, Gruswitz F. HOLLOW: generating accurate representations of channel and interior surfaces in molecular structures. BMC Struct Biol. 2008; 8:49. [PubMed: 19014592]

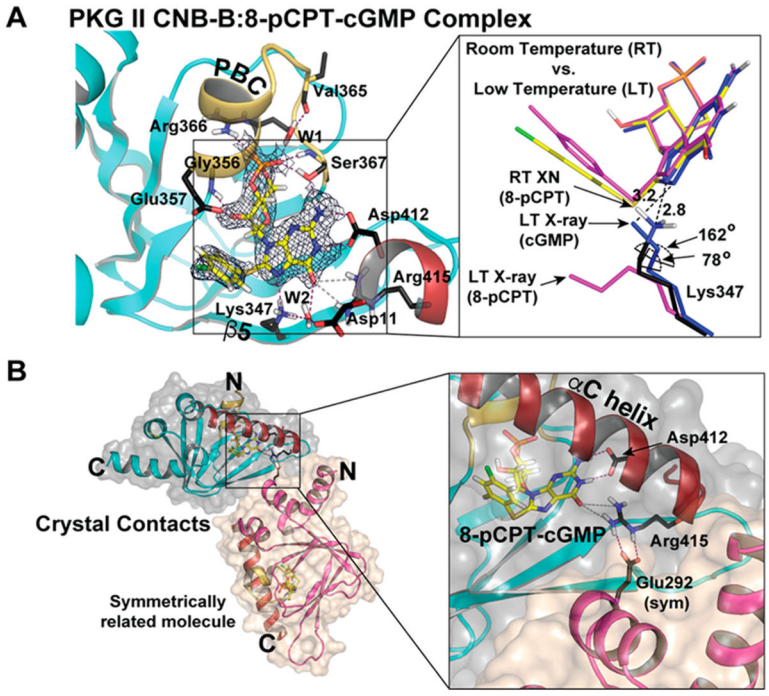

Figure 1.

Interactions between the PKG II CNB-B domain and 8-pCPT-cGMP. (A) 8-pCPT cGMP binding pocket. CNB-B is colored light teal excluding the PBC and the αC helix, which are colored yellow and red, respectively. 8-pCPT-cGMP is shown as sticks and colored by atom type (carbon, yellow; nitrogen, blue; oxygen, red; phosphorus, orange). Key cGMP-interacting residues are colored by atom type with carbon colored black. O···O and O···N distances are shown as dashed lines with units of angstroms. The $2F_O - F_C$ nuclear density map (blue mesh) is shown at 1.1σ for bound 8-pCPT-cGMP. A close-up view shows different side chain conformations of Lys347 seen in the RT XN and LT X-ray structures with 8-cCPT-cGMP bound and the LT X-ray structure with cGMP bound. The LT X-ray structure bound with cGMP (PDB entry 5BV6) is colored blue. The LT X-ray structure bound with 8-pCPT-cGMP (PDB entry 5JIZ) is colored magenta. (B) Crystal contacts in the RT XN structure of PKG II CNB-B:8-pCPT-cGMP between Arg415 and Glu292(sym). The side chains of Arg415 and Glu292(sym) form a salt bridge. PKG II CNB-B domains are shown with a transparent surface, with the molecule at the origin colored gray and the symmetry-related molecule colored tan.

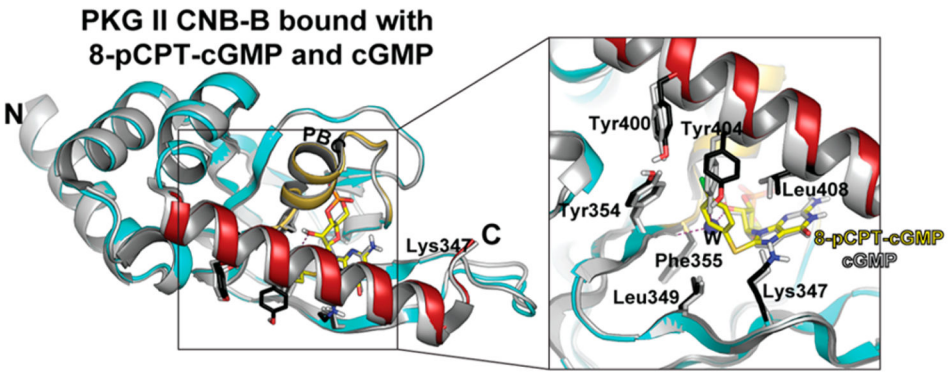

Figure 2.

Structural changes of the PKG II CNB-B domain associated with 8-pCPT-cGMP binding. Superposition of the XN PKG II CNB-B:8-pCPT-cGMP and LT X-ray PKG II CNB-B:cGMP complexes. The XN PKG II:8-pCPT-cGMP is shown with the same color theme as in Figure 1. Key binding residues are shown as sticks. Both termini are labeled. The LT X-ray structure is colored gray.

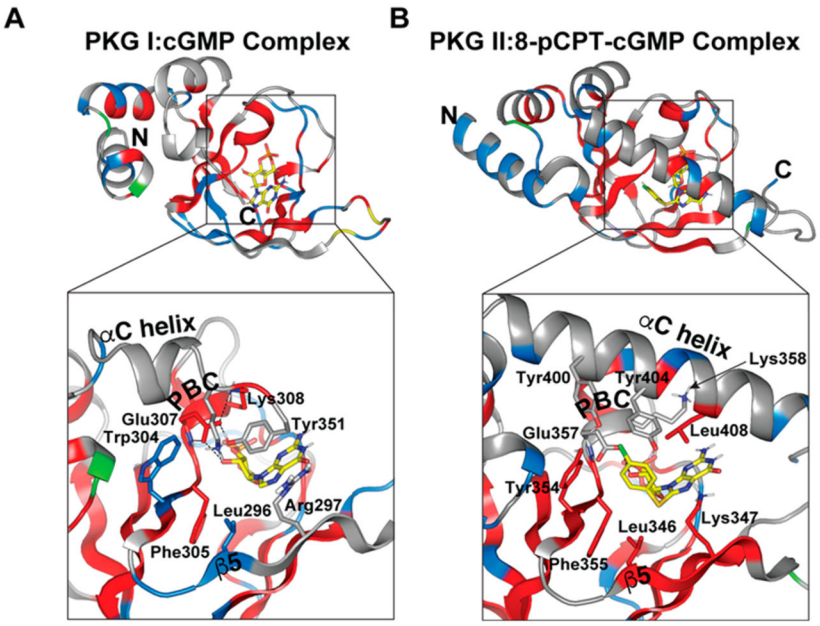

Figure 3.

Backbone amide H/D exchange patterns in (A) PKG Iβ:cGMP and (B) PKG II:8-pCPT-cGMP complexes. N- and C-termini are labeled. Fully exchanged amides are colored gray, partially exchanged amides blue, and nonexchanged amides red. Proline residues are colored green. Close-up views show key binding residues.

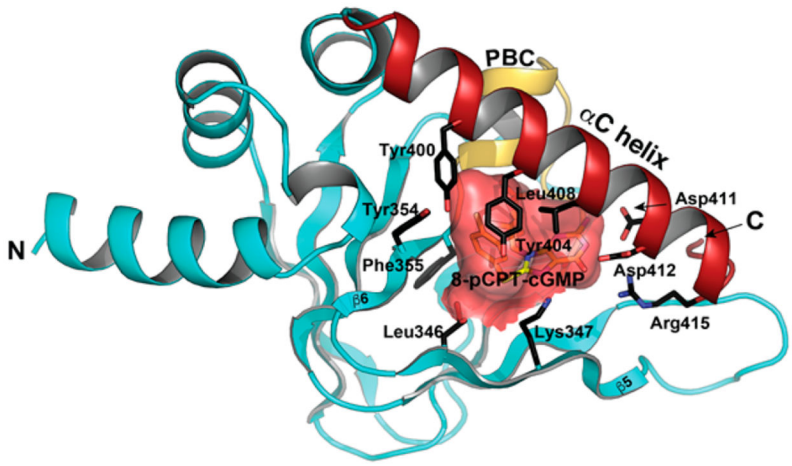

Figure 4.

8-pCPT-cGMP binding pocket. The surface of the binding pocket is colored red. The binding pocket was calculated using Hollow.[21]

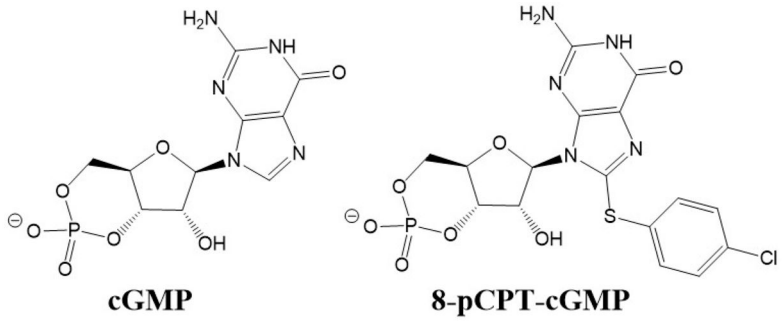

Scheme 1.
Chemical Diagrams of cGMP and 8-pCPT-cGMP